Appl. Phys. A (2016)122:346
DOI 10.1007/s00339-016-9935-8

Applied Physics A
Materials Science & Processing

Irradiation with visible light enhances the antibacterial toxicity of silver nanoparticles produced by laser ablation

Matthew Ratti[1] · J. J. Naddeo[1] · Yuying Tan[1] · Julianne C. Griepenburg[1] · John Tomko[1] · Cory Trout[1] · Sean M. O'Malley[1,2] · Daniel M. Bubb[1,2] · Eric A. Klein[2,3]

Received: 29 October 2015 / Accepted: 23 February 2016

Abstract The rise of antibiotic-resistant bacteria is a rapidly growing global health concern. According to the Center for Disease Control, approximately 2 million illnesses and 23,000 deaths per year occur in the USA due to antibiotic resistance. In recent years, there has been a surge in the use of metal nanoparticles as coatings for orthopedic implants, wound dressings, and food packaging, due to their antimicrobial properties. In this report, we demonstrate that the antibacterial efficacy of silver nanoparticles (AgNPs) is enhanced with exposure to light from the visible spectrum. We find that the increased toxicity is due to augmented silver ion release and bacterial uptake. Interestingly, silver ion toxicity does not appear to depend on the formation of reactive oxygen species. Our findings provide a novel paradigm for using light to regulate the toxicity of AgNPs which may have a significant impact in the development of new antimicrobial therapeutics.

1 Introduction

The ever-increasing challenge of multidrug resistance in bacteria requires the identification of novel drug targets as well as innovative drug delivery mechanisms. One new focus of antimicrobial research revisits a centuries-old medical technology—antibacterial metals [1]. Today, nanomaterial technology enables the production of 1–100-nm-sized particles of metals and metal oxides which are finding uses in coatings for medical devices and bacteria-resistant packaging. Numerous strategies have been proposed to regulate the efficacy and toxicity of nanoparticles (NPs) including size, metal composition, and oxidation state (reviewed in [2]). Additionally, several studies have demonstrated photocatalytic toxicity of TiO_2 nanoparticles toward bacteria [3–5]; doping TiO_2 particles with silver further increases their photocatalytic antibacterial efficacy [6]. In this study, we investigate light-enhanced antimicrobial properties of silver nanoparticles (AgNPs) and their underlying mechanism of action.

2 Experimental details

2.1 AgNP synthesis by pulsed laser ablation in liquids (PLAL)

AgNPs were synthesized by adhering a silver target to a porous stage with carbon tape to reduce movement during the ablation process. A magnetic stir bar was placed under the stage to help reduce secondary irradiation of particles produced by the previous laser pulse and to reduce the production of temperature and concentration gradients [7]. The target and stage were then carefully lowered into a 50-ml Pyrex beaker containing 40 ml of either 60 mM

Matthew Ratti and J. J. Naddeo have contributed equally to this work.

✉ Eric A. Klein
eric.a.klein@rutgers.edu

[1] Physics Department, Rutgers University-Camden, Camden, NJ 08102, USA

[2] Center for Computational and Integrative Biology, Rutgers University-Camden, Camden, NJ 08102, USA

[3] Biology Department, Rutgers University-Camden, Camden, NJ 08102, USA

Published online: 10 March 2016

sodium dodecyl sulfate (SDS; Fisher Scientific) or 2 mM polyvinylpyrrolidone (PVP; Sigma). Laser ablation was carried out via a Nd:YAG laser (Ekspla NL-303) operating at the fundamental wavelength of 1064 nm, with a pulse duration of approximately 5 ns, and running at a repetition rate of 10 Hz. The energy per pulse was measured with a Laser Power and Energy Meter. The beam was focused using a converging lens with a focal length of 250 mm yielding a spot size with an average area of 5.51 mm^2. The colloidal solution was made in complete darkness to avoid any interactions between ambient light and the produced AgNPs. The UV–Vis spectrum (200–1100 nm) was measured using a Cary 60 Spectrophotometer. In order to obtain a clean spectrum, we measured the produced solutions by diluting them 1:10. The hydrodynamic diameter of the primary particles was measured using a Malvern Zetasizer Nano Series dynamic light scattering unit. This measurement was made to ensure the absence of any particles with dimensions greater than 100 nm. Size measurements of SDS-coated AgNPs were also made using a Zeiss EM902 transmission electron microscope. AgNP concentration was determined by weighing the silver target before and after ablation using a microbalance (Sartorius Cubis MSU). Any difference in weight was assumed to be transferred to the solution in the form of AgNPs. AgNPs were synthesized and stored in complete darkness to prevent light-induced ion release. Additionally, to prevent temperature induced ion release and/or aggregation, the samples were stored at room temperature; storage below room temperature results in SDS precipitation and unwanted particle aggregation.

2.2 Bacterial culture

Except for the bioavailability assays, all experiments were performed using the K-12 *E. coli* strain MG1655 or *B. subtilis* strain W168. Bioavailability assays were performed using *E. coli* strain MC1061 (pSLcueR/pDNPcopAlux), a kind gift from Anne Kahru (National Institute of Chemical Physics and Biophysics, Estonia) [9]. All strains were cultured in lysogeny broth (LB) media (10 g l^{-1} bacto-tryptone (BD Bioscience), 5 g l^{-1} yeast extract (BD Bioscience), and 10 g l^{-1} sodium chloride (Sigma)). LB-agar plates contained 15 g l^{-1} bacto-agar (BD Bioscience). Where appropriate, antibiotic concentrations for liquid cultures were: tetracycline (12 μg ml^{-1}; Fisher Scientific); carbenicillin (50 μg ml^{-1}; Caisson Labs). All strains were grown at 37 °C with shaking at 250 RPM.

2.3 Determining AgNPs toxicity in *E. coli* and *B. subtilis*

Overnight cultures of *E. coli* were diluted to an optical density ($\lambda = 600$ nm) of 0.01 into clear glass tubes containing LB media with 10 mM SDS. SDS was included in the LB media so that the total SDS concentration remained constant upon the addition of AgNPs. *B. subtilis* cultures were prepared similarly; however, no SDS was added to the media due to its toxicity against this organism. AgNPs (SDS preparations for *E. coli* and PVP preparations for *B. subtilis*) were added in the dark to prevent unwanted photoinduced ion release. Test tubes used for "dark" samples were covered in aluminum foil. Kanamycin (30 μg ml^{-1}; Fisher Scientific), a bactericidal antibiotic, was used as a positive control. The test tubes were then placed into an incubator shaker at 37 °C and 250 RPM. The incubator shaker was fitted with an LED source. The LED was set to emit red, green, and blue light simultaneously at low intensity (1.768 mW cm^{-2}), as measured with a Thorlabs Silicon detector (DET10A). After a 2-h (*E. coli*) or 9-h (*B. subtilis*) incubation, an aliquot from each test tube was taken and serial dilutions were plated onto LB-agar media to measure colony forming units (cfu).

2.4 Dead-cell staining and microscopy

Following AgNP treatment, *E. coli* cells were stained with 2.5 μg ml^{-1} propidium iodide (Invitrogen) for 5 min at room temperature. Cells were seeded onto 1 % agarose pads and imaged at 100× (NA 1.45) by phase contrast and fluorescence microscopy on a Nikon TiE microscope equipped with a Zyla sCMOS camera.

2.5 Determining soluble silver ion concentration

The sulfur-containing organic ligand, dithizone (Sigma), forms a complex with Ag^+ ions with an absorption peak at roughly 465 nm [8]. To measure light-induced Ag^+ ion release, AgNPs were synthesized using PLAL in complete darkness. The sample was clarified using a 1-μm filter and split into two vials. One vial was wrapped in foil to avoid exposure to ambient light, while the other was placed into a clear glass test tube. Both light and dark samples were placed in front of the LED source in the incubator shaker at 37 °C and 250 RPM for 2 h. The AgNPs in both solutions were pelleted at 287,660 × g for 12 h, and the supernatant was collected. No SPR was observed in the UV–Vis spectra so it was assumed that there was not an appreciable amount of AgNPs present in the supernatant. UV–Vis spectra of each sample were measured (350–700 nm) to assess changes in peak height for the characteristic absorbance of the Ag^+-dithizone complex.

2.6 Quantification of Ag^+ bioavailability

Silver bioavailability was measured using an engineered *E. coli* strain harboring plasmids encoding the silver sensing response element (*cueR*) and luciferase under the

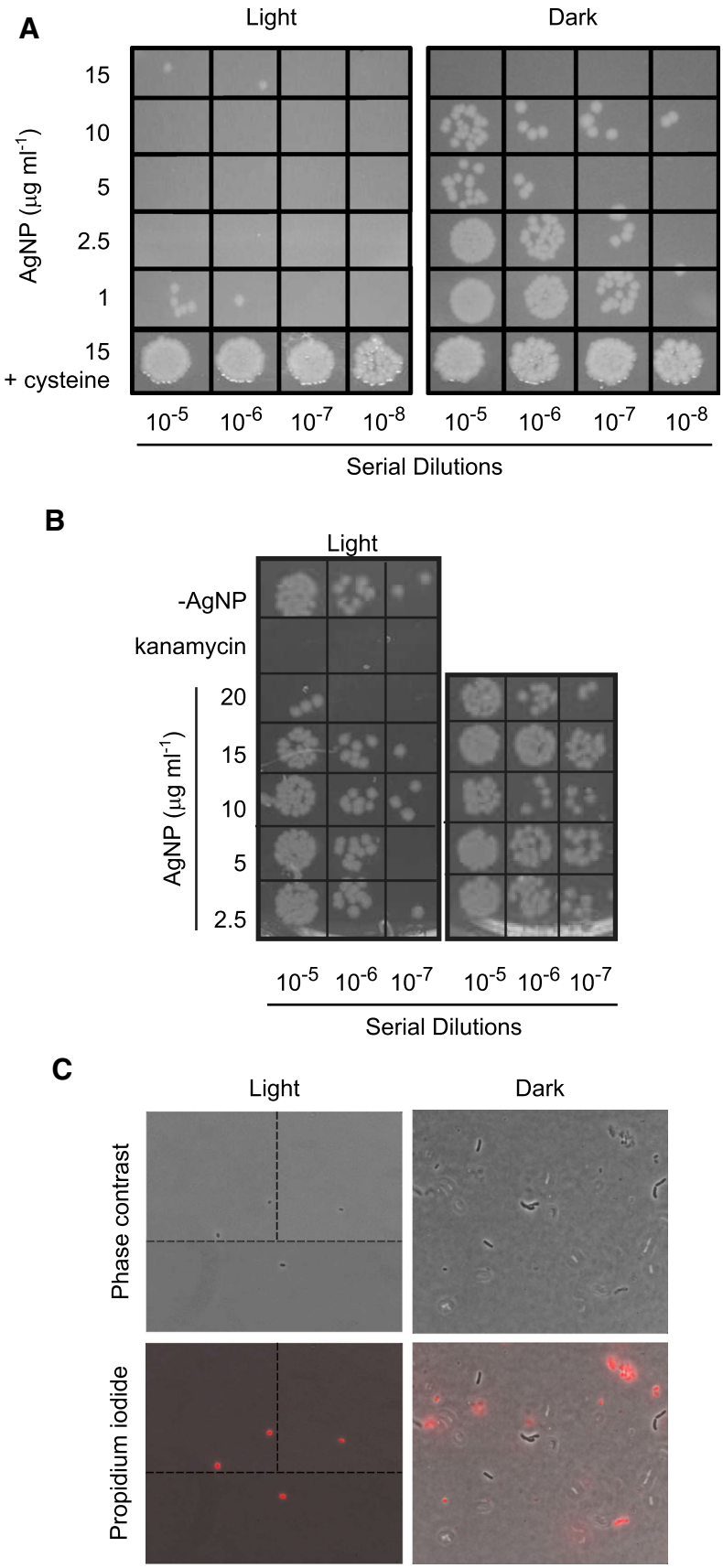

Fig. 1 Irradiation of AgNPs with *white light* enhances antibacterial toxicity. **a** *E. coli* cells were treated for 2 h with varying concentrations of AgNPs. Duplicate cultures were incubated either exposed to *light* or in the *dark*. Serial dilutions of cultures were plated on LB-agar to determine bacterial viability. Bactericidal effects of AgNPs were blocked by treatment with 3.3× molar excess cysteine. Image is a representative experiment (AgNP treatment $n = 5$; cysteine recovery $n = 3$). **b** *B. subtilis* cells were treated for 9 h with varying concentrations of AgNPs. Duplicate cultures were incubated either exposed to *light* or in the *dark*. Kanamycin treatment (10 μg ml^{-1}) was included as a positive control, and untreated cells served as a negative control. Serial dilutions of cultures were plated on LB-agar to determine bacterial viability. Image shows a representative experiment ($n = 3$). **c** *E. coli* cells were treated with 15 μg ml^{-1} AgNPs in the *light* or *dark* for 2 h and stained with propidium iodide (*red fluorescence*) to label dead cells. *Black dashed lines* indicate where several image fields were stitched together. Images display representative cells (*dark* treatment: >100 cells imaged; *light* treatment: AgNP toxicity is very high, thus very few cells (<10) were present in culture)

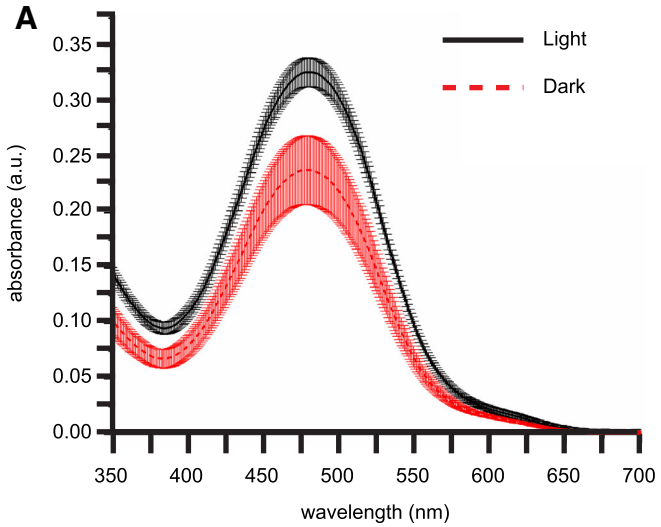
A
Light
Dark
absorbance (a.u.)
0.35
0.30
0.25
0.20
0.15
0.10
0.05
0.00
350
400
450
500
550
600
650
700
wavelength (nm)

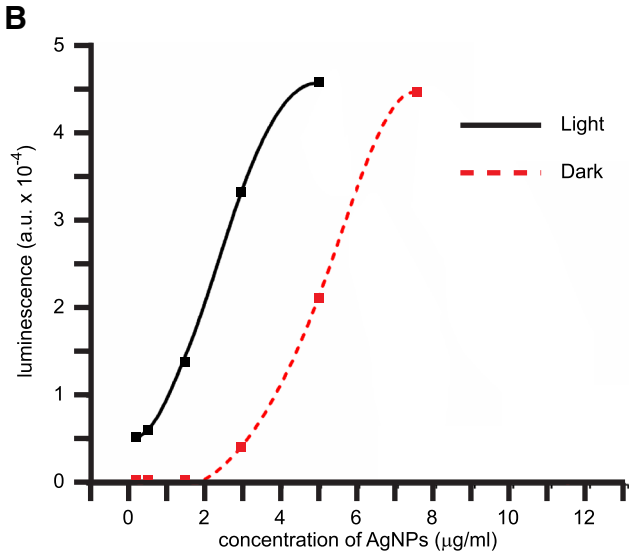
B
Light
Dark
luminescence (a.u. x 10^-4)
5
4
3
2
1
0
0
2
4
6
8
10
12
concentration of AgNPs (μg/ml)

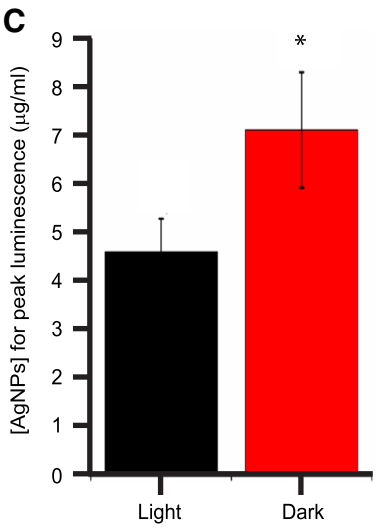
C
*
[AgNPs] for peak luminescence (μg/ml)
9
8
7
6
5
4
3
2
1
0
Light
Dark

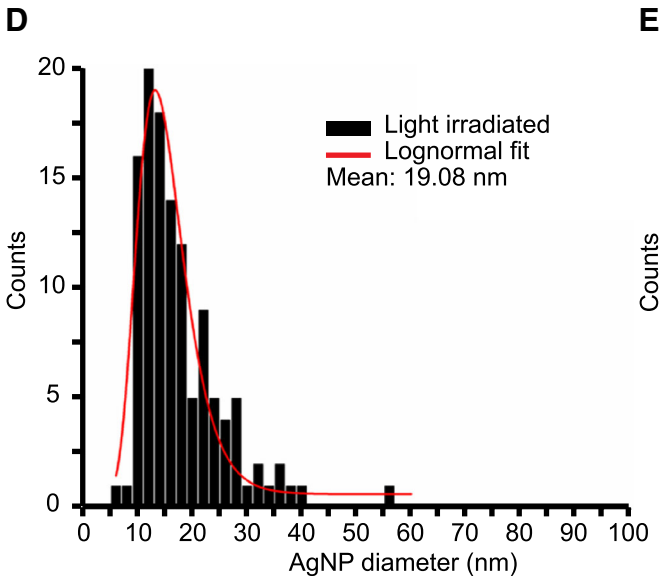
D
Light irradiated
Lognormal fit
Mean: 19.08 nm
Counts
20
15
10
5
0
0
10
20
30
40
50
60
70
80
90
100
AgNP diameter (nm)

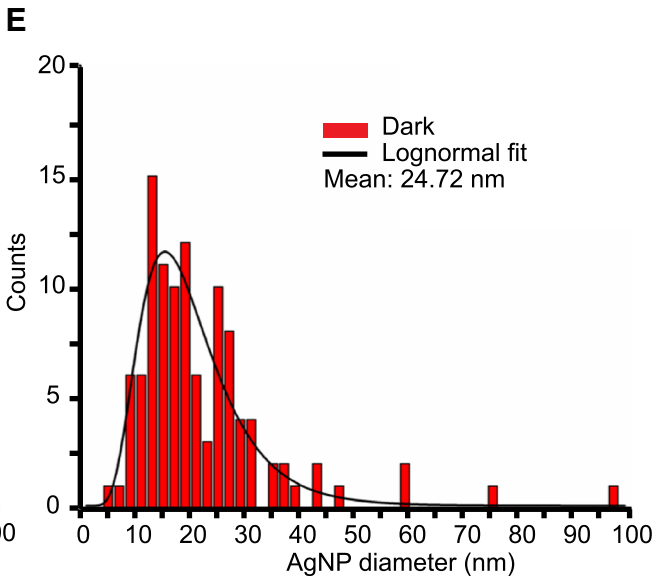
E
Dark
Lognormal fit
Mean: 24.72 nm
Counts
20
15
10
5
0
0
10
20
30
40
50
60
70
80
90
100
AgNP diameter (nm)

◀**Fig. 2** Irradiation of AgNPs increases release of silver ions. **a** AgNPs were either irradiated by LED *light* for 2 h or maintained in the *dark*. Soluble silver ions were measured using the dithizone assay ($n = 3$). **b** A bioluminescent silver-reporter strain (MC1061) was used to measure silver bioavailability. Cells were incubated with increasing concentrations of AgNPs in either *light* or *dark* conditions, and luminescence was quantified and normalized to optical density ($\lambda = 600$ nm) (representative experiment, $n = 5$). **c** The concentration of AgNPs required for peak luminescence was determined for $n = 5$; *error bars* are 1σ ($\sigma_{dark} = 1.19$ $\sigma_{light} = 0.68$). $^{*}p = 0.005$. **d–e** The sizes of AgNPs were measured by TEM with or without light exposure

control of the *copA* promoter (strain, MC1061 pSLcueR/pDNPcopAlux). To measure silver bioavailability, the reporter strain was grown overnight in LB with tetracycline and carbenicillin at 37 °C. The overnight culture was diluted 1:50 into fresh media and grown to OD600 = 0.1. Bacteria were then transferred to glass tubes (2 ml per tube) and supplemented with 2 ml of varying concentrations of AgNPs. The tubes were incubated at 37 °C and shaken at 250 RPM for 2 h either exposed to LED illumination or in the dark. 200 µl aliquots from each tube were then transferred to a white 96-well plate to measure the resulting luminescence. 200 µl were also transferred to a clear 96-well plate to measure the optical density at 600 nm. Luminescence and absorbance were measured on a BMG Labtech CLARIOstar plate reader.

3 Results

3.1 Production of silver nanoparticles by pulsed laser ablation in liquids

Silver nanoparticles used in this study were prepared by utilizing the pulsed laser ablation in liquids (PLAL) method [8] resulting in deep amber colloidal solutions with an extinction peak centered at ~400 nm. This peak is characteristic of the surface plasmon resonance (SPR) band of AgNPs suspended in an aqueous environment [9]. The solutions remained stable for months, as evidenced by minimal changes in their UV–Vis spectra and the absence of any observable sedimentation. AgNPs primarily interact with UV and visible light through the excitation of free carriers and surface plasmons. These excited electrons facilitate redox reactions at the interface between the nanoparticle and the surrounding medium [10]. Therefore, AgNP solutions were synthesized and stored in complete darkness.

3.2 Light enhances antibacterial properties of AgNPs

Several studies have demonstrated photocatalytic toxicity of TiO_2 nanoparticles toward bacteria [3–5]. Furthermore, doping TiO_2 particles with silver increases their photocatalytic antibacterial efficacy [6]. To determine whether light similarly enhances the antimicrobial properties of AgNPs alone, overnight cultures of *E. coli* were diluted into fresh lysogeny broth (LB) media in glass culture tubes and treated with AgNPs at concentrations ranging from 0 to 15 µg/ml. The *E. coli* cultures were grown for 2 h while exposed to an RGB LED source ($I = 1.8$ mW cm^{-2}). Identically prepared cultures were grown in dark conditions by wrapping the selected tubes in aluminum foil. After 2 h, cultures were serially diluted and plated on LB-agar media to measure colony-forming units (cfu). AgNP toxicity was observed in dark cultures at concentrations of 15 µg ml^{-1}, whereas those exposed to light, in otherwise identical conditions, effectively killed *E. coli* at 1 µg ml^{-1}

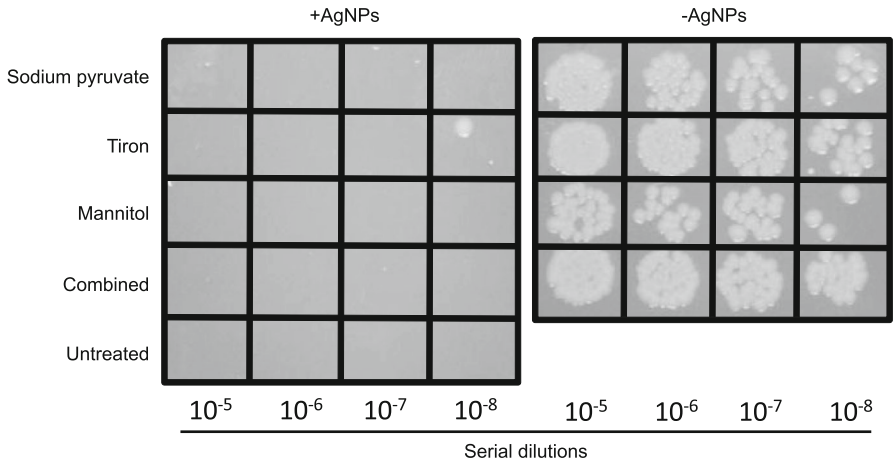

Fig. 3 Toxicity of AgNPs is not dependent on ROS production. *E. coli* cells were incubated for 2 h with 15 µg ml^{-1} AgNPs and light exposure. Cultures were treated with various ROS scavengers: sodium pyruvate (H_2O_2; 50 mM), tiron ($\cdot O_2^-$; 50 mM) and mannitol ($\cdot$OH; 100 mM). A combination of all 3 ROS scavengers included 10 mM sodium pyruvate, 10 mM tiron, and 50 mM mannitol. Serial dilutions of cultures were plated on LB-agar to determine bacterial viability. Image shows a representative experiment ($n = 3$)

(Fig. 1a). Light-enhanced toxicity is not limited to Gram-negative organisms; indeed, we observed a similar increase in toxicity of irradiated samples when treating the Gram-positive species *B. subtilis* with 20 μg ml^{-1} AgNPs (Fig. 1b). This enhanced cell death was attributed to nanoparticle-induced phototoxicity, as cells exposed to light in the absence of AgNPs showed no decrease in viability. The bactericidal effects of AgNPs were confirmed by staining with the membrane-impermeable dead-cell stain, propidium iodide (PI). Cells treated with AgNPs in the light were round and stained uniformly with PI (Fig. 1c). In contrast, *E. coli* grown with AgNPs in the dark displayed a wide range of cell morphologies and variable PI staining.

3.3 Irradiation of AgNPs stimulates silver ion release

A number of studies have reported that AgNP bacterial toxicity is due to silver ion release [11, 12]. We assayed photoinduced Ag^+ release using a colorimetric assay based on a characteristic dithizone-Ag^+ absorbance peak [13]. The relative Ag^+ ion concentration increased by 31 ± 8.5 % upon light exposure (Fig. 2a). Additionally, in order to determine whether the elevated ion concentration resulted in higher intracellular Ag^+ concentrations we used a silver-sensitive luciferase reporter [14], which revealed a 40 % increase in intracellular ion concentration (Fig. 2b, c). These results are consistent with one another and strongly suggest photoactivated release of Ag^+ ions.

It has been shown recently that AgNPs release ions due to an increase in thermal energy and that released Ag^+ ions are able to nucleate to form small AgNPs (<10 nm in diameter) [15, 16]. Additionally, the heat dissipation by NPs trends with size as R^{-2}, where R is the radius of the NP; absorption of incident light is much stronger in larger NPs (~40–50 nm in diameter) than in smaller NPs (<10 nm in diameter) [17, 18]. TEM analysis demonstrates that irradiation of AgNPs results in a lower mean particle diameter ($p = 0.0035$) (Fig. 2d, e). This can be explained by the aforementioned size relationship that suggests larger AgNPs selectively absorb a majority of the incident photons and, due to an increase in thermal energy, release Ag^+ ions that later nucleate, thus increasing the population of smaller AgNPs.

3.4 Soluble silver ions are the primary antibacterial agent of AgNPs

To determine whether the light-dependent increase in ion release and bioavailability directly mediate the antibacterial effects of AgNPs, we chelated released Ag^+ ions with L-cysteine [19]. Silver chelation completely inhibited AgNP toxicity in both light and dark conditions (Fig. 1a; bottom row). Interestingly, these ion-mediated effects appear to be independent of reactive oxygen species (ROS), since the addition of several ROS inhibitors did not affect AgNP efficacy (Fig. 3).

4 Discussion and conclusions

Our results demonstrate that AgNPs display a light-enhanced antimicrobial activity. This toxicity is specifically due to increased Ag^+ ion release and bacterial uptake; this differs from the light-induced antimicrobial activity of TiO_2 which is ROS mediated [20–22]. These results provide a novel platform for developing spatially and temporally regulated nanoparticle-based coatings and therapeutics. For example, a topical AgNP-based antibiotic could be precisely activated at the site of a wound using white-light irradiation. Tight control of AgNP activity may be used to limit collateral damage to surrounding tissue.

It should be noted that these findings appear to contradict recent reports suggesting that visible light (1) reduces AgNP ion release in an environment with dissolved organic matter and (2) decreases AgNP toxicity toward the eukaryotic organism *Tetrahymena pyriformis* [23, 24]. While these results may reflect environmental differences or a difference between eukaryotic and prokaryotic biology, another explanation is that the observed disparities are a result of the methods used in AgNP synthesis. AgNP dissolution and agglomeration is dependent on surface coating [25]. Thus, our results using PLAL with SDS or PVP to stabilize particles suggest that this particular surfactant may enhance AgNP ion release and toxicity in response to irradiation.

Acknowledgments This work was supported by the National Science Foundation (NSF awards CMMI-0922946 to D.B. and CMMI-1300920 to D.B. and S.O'M.) and a Busch Biomedical Research Grant to E.K. and S.O'M.

References

1. J.W. Alexander, History of the medical use of silver. Surg. Infect. (Larchmt) **10**, 289–292 (2009)
2. J.A. Lemire, J.J. Harrison, R.J. Turner, Antimicrobial activity of metals: mechanisms, molecular targets and applications. Nat. Rev. Microbiol. **11**, 371–384 (2013)
3. J.-S. Hur, Y. Koh, Bactericidal activity and water purification of immobilized TiO2 photocatalyst in bean sprout cultivation. Biotechnol. Lett. **24**, 23–25 (2002)
4. A.-G. Rincon, C. Pulgarin, Effect of pH, inorganic ions, organic matter and H2O2 on *E. coli* K12 photocatalytic inactivation by TiO2: implications in solar water disinfection. Appl. Catal. B **51**, 283–302 (2004)

5. J.C. Yu, W. Ho, J. Lin, H. Yip, P.K. Wong, Photocatalytic activity, antibacterial effect, and photoinduced hydrophilicity of TiO2 films coated on a stainless steel substrate. Environ. Sci. Technol. **37**, 2296–2301 (2003)
6. K. Gupta, R.P. Singh, A. Pandey, A. Pandey, Photocatalytic antibacterial performance of TiO2 and Ag-doped TiO2 against *S. aureus*. *P. aeruginosa* and *E. coli*. Beilstein J. Nanotechnol. **4**, 345–351 (2013)
7. S. Barcikowski, A. Menndez-Manjon, B. Chichkov, M. Brikas, G. Raciukaitis, Generation of nanoparticle colloids by picosecond and femtosecond laser ablations in liquid flow. Appl. Phys. Lett. **91**, 083113 (2007)
8. V. Amendola, M. Meneghetti, What controls the composition and the structure of nanomaterials generated by laser ablation in liquid solution? Phys. Chem. Chem. Phys. **15**, 3027–3046 (2013)
9. S.L. Smitha, K.M. Nissamudeen, D. Philip, K.G. Gopchandran, Studies on surface plasmon resonance and photoluminescence of silver nanoparticles. Spectrochim. Acta A Mol. Biomol. Spectrosc. **71**, 186–190 (2008)
10. X. Chen, Z. Zheng, X. Ke, E. Jaatinen, T. Xie, D. Wang, C. Guo, J. Zhao, H. Zhu, Supported silver nanoparticles as photocatalysts under ultraviolet and visible light irradiation. Green Chem. **12**, 414–419 (2010)
11. G.A. Sotiriou, S.E. Pratsinis, Antibacterial activity of nanosilver ions and particles. Environ. Sci. Technol. **44**, 5649–5654 (2010)
12. Z.-M. Xiu, Q.-B. Zhang, H.L. Puppala, V.L. Colvin, P.J.J. Alvarez, Negligible particle-specific antibacterial activity of silver nanoparticles. Nano Lett. **12**, 4271–4275 (2012)
13. M. Reza, V. Hosseini, F. Shamsa, H. Jamalifar, Preparation and in vitro antibacterial evaluation of electroless silver coated polymers. Iran. J. Pharm. Res. (IJPR) **9**, 259–264 (2010)
14. A. Ivask, T. Rolova, A. Kahru, A suite of recombinant luminescent bacterial strains for the quantification of bioavailable heavy metals and toxicity testing. BMC Biotechnol. **9**, 41 (2009)
15. S. Kittler, C. Greulich, J. Diendorf, M. Koller, M. Epple, Toxicity of silver nanoparticles increases during storage because of slow dissolution under release of silver ions. Chem. Mater. **22**, 4548–4554 (2010)
16. X. Li, J.J. Lenhart, Aggregation and dissolution of silver nanoparticles in natural surface water. Environ. Sci. Technol. **46**, 5378–5386 (2012)
17. V. Amendola, M. Meneghetti, Laser ablation synthesis in solution and size manipulation of noble metal nanoparticles. Phys. Chem. Chem. Phys. **11**, 3805–3821 (2009)
18. M. Hu, G.V. Hartland, Heat dissipation for Au particles in aqueous solution: relaxation time versus size. J. Phys. Chem. B **106**, 7029–7033 (2002)
19. S.Y. Liau, D.C. Read, W.J. Pugh, J.R. Furr, A.D. Russell, Interaction of silver nitrate with readily identifiable groups: relationship to the antibacterial action of silver ions. Lett. Appl. Microbiol. **25**, 279–283 (1997)
20. J.F. Reeves, S.J. Davies, N.J. Dodd, A.N. Jha, Hydroxyl radicals (*OH) are associated with titanium dioxide (TiO(2)) nanoparticle-induced cytotoxicity and oxidative DNA damage in fish cells. Mutat. Res. **640**, 113–122 (2008)
21. C.M. Sayes, R. Wahi, P.A. Kurian, Y. Liu, J.L. West, K.D. Ausman, D.B. Warheit, V.L. Colvin, Correlating nanoscale titania structure with toxicity: a cytotoxicity and inflammatory response study with human dermal fibroblasts and human lung epithelial cells. Toxicol. Sci. **92**, 174–185 (2006)
22. B. Shen, J.C. Scaiano, A.M. English, Zeolite encapsulation decreases TiO2-photosensitized ROS generation in cultured human skin fibroblasts. Photochem. Photobiol. **82**, 5–12 (2006)
23. J. Shi, B. Xu, X. Sun, C. Ma, C. Yu, H. Zhang, Light induced toxicity reduction of silver nanoparticles to *Tetrahymena Pyriformis*: effect of particle size. Aquat. Toxicol. **132–133**, 53–60 (2013)
24. Y. Yin, J. Liu, G. Jiang, Sunlight-induced reduction of ionic Ag and Au to metallic nanoparticles by dissolved organic matter. ACS Nano **6**, 7910–7919 (2012)
25. Y. Li, W. Zhang, J. Niu, Y. Chen, Surface-coating-dependent dissolution, aggregation, and reactive oxygen species (ROS) generation of silver nanoparticles under different irradiation conditions. Environ. Sci. Technol. **47**, 10293–10301 (2013)